Biomacromol. J. Vol. 2, No. 2, 152-161, December 2016.

Biomacromolecular Journal
www.bmmj.org

Water-based Double Layer Functionalized Iron Oxide Nanoparticles for Enhanced Gene Delivery Applications

S. Khoshnevis[a], Z. Hassani[b,a,*], M. Torkzadeh-Mahani[c] and M. Mahani[a]

[a]*Department of Chemistry and Nanochemistry, Faculty of Sciences & Modern Technologies, Graduate University of Advanced Technology, P.O. Box: 76315-117, Kerman, Iran*

[b]*Department of New Materials, Institute of Science, High Technology and Environmental Sciences, Graduate University of Advanced Technology, P.O. Box: 76315-117, Kerman, Iran*

[c]*Department of Biotechnology, Institute of Science, High Technology and Environmental Sciences, Graduate University of Advanced Technology, P.O. Box: 76315-117, Kerman, Iran*

(Received 3 March 2017, Accepted 8 May 2017)

ABSTRACT

Iron oxide nanoparticles (magnetite (Fe_3O_4), hematite (Fe_2O_3)) have been received increasing attention in drug and gene delivery. In this work, water-base double layer functionalized iron oxide nanoparticles (DL-IONPs) were designed and prepared of a biodegradable, biocompatible carrier by co-precipitation method with high DNA loading capacity due to self-assembly of a second organic layer. The prepared nanocarriers were characterized by FTIR spectra, XRD, dynamic light scattering and vibrating sample magnetometry. Gene loading ability of the nanocarriers was determined using gel retardation electrophorese method. Finally, cytotoxicity and transfection assays toward HEK293T cell line were studied. Several advantages compared to other systems are simple synthesis procedure, high ability for condensation of nucleic acids due to positive charge around of carrier and suitable capacity for loading hydrophobic drugs in consequences of the hydrophobic area formation between the first and second layers. Results from gel retardation assay demonstrated that the DNA can efficiently attach to DL-IONPs particles, and protect plasmid DNA from nucleases attack and degradation.

Keywords: Functionalized iron oxide nanoparticles, Gene delivery, Nanocarriers, *HEK* 293 cells, Transfection assay

INTRODUCTION

Various transfection methods for gene and drug delivery on the basis of synthetic carriers such as nanoparticles, polymers, liposomes and dendrimers have been developed. Nevertheless, designing and preparation of a biodegradable, biocompatible carrier, and especially smart delivery system is a challenge. In the last decades, magnetic nanoparticles due to their unique properties have received many attentions in imaging and gene delivery applications [1].

The use of magnetic micro particles for gene delivery was firstly demonstrated by CathrynMah, *et al*. [2], for *in vitro* transfection in C12S cells and in vivo transfection in mice using adeno associated virus (AAV) linked to magnetic microspheres *via* heparin[2].

*Corresponding author. E-mail: hassanizahra@yahoo.com

Amongst magnetic nanoparticles (MNPs), Fe_3O_4 has been used extensively, because of biocompatibility, high moment at low magnetic field, super paramagnetic property and stability at physiological conditions [3]. Super paramagnetic iron oxide nanoparticles (SP-IONPs) with appropriate surface chemistry and unique magnetic properties can be used for numerous applications, such as magnetic resonance imaging (MRI) contrast enhancement [4], hyperthermia [5], drug and gene delivery [6,7].

The synthesis of iron oxide nanoparticles (IONPs) is facile and affordable; moreover, produced nanoparticles have unique and size-dependent magnetic properties [8]. This phenomenon appears at the nano scale when the dimensions of a ferromagnetic material are reduced below to the typical size of magnetic domains, that generally known as superparamagnetism. Suspensions of SP-IONPs, generally referred as Ferro-fluids, are essentially

paramagnetic liquids which are useful in biomedical applications such as MRI, sensing, diagnosis, magnetic separation and drug and gene delivery [9,10].

The controlled synthesis of SP-IONPs was firstly by Massart [9,11]. Various chemical methods for synthesis of iron oxide nanoparticles have been used including sonochemical reactions [12-14], microemulsions [15], co-precipitation [11,16,17], hydrothermal reactions [18-20], thermal decomposition [21], and sol-gel synthesis [22]. It is generally accepted that the best synthetic route for the preparation of iron oxide cores is based on high-temperature decomposition of organic precursors which results in narrow size distribution, with a well-defined shape and good crystallinity. However, the drawback of this method is that the nanoparticles (NPs) are surfactant coated and water insoluble [23].

The co-precipitation method is the simplest, most common and efficient chemical method for obtaining magnetic nanoparticles. In this method, iron oxide NPs are produced by reduction of a mixture of ferrous and ferric salts in aqueous medium. Fe_3O_4 is synthesized in the pH range of 8-14 in reducing medium [24,25].

Because of limited reactivity, direct conjugation of biomolecules to IONPs surface is not common. More commonly, IONPs surface is functionalized by a layer of intermediate molecules such as hydroxyl groups, diols, phosphates, dithiols and carboxylates that prepare a substrate for further conjugation [9].

In this work, water-base double layer functionalized iron oxide nanoparticles (DL-IONPs) were synthesized by co-precipitation method and self-assembly of a second organic layer. CTAB and SDS were used for bilayer-type and water soluble structure formation. Most important advantages of this method are simple synthesis procedure, high ability for condensation of nucleic acids due to positive charge around of carrier and suitable capacity for loading hydrophobic drugs in consequences of the hydrophobic area formation between the first and second layers. The synthesized DL-IONPs were characterized by FTIR spectra, X-ray diffractometer (XRD), dynamic light scattering (DLS) and vibrating sample magnetometry (VSM). Their cytotoxicity in the human HEK293T cell line were evaluated. Finally magnetic nanoparticles were experienced toward HEK293T cell line for assessment of their ability for gene transfection.

EXPERIMENTAL

Materials

Iron(III) chloride hexahydrate ($FeCl_3.6H_2O$) (97%), Iron(II) chloride tetrahydrate ($FeCl_2.4H_2O$) (≥99.0%), Sodium Dodecyl Sulfate (SDS) (≥99.5%) were purchased from Sigma-Aldrich. Hydrochloric acid 37%, Ammonia Solution 25% and Oleic Acid were purchased from Merck. All of the chemicals were used without any purification as received.

Preparation of Oleic Acid Capped IONPs

Iron oxide nanoparticles were synthesized by co-precipitation method. Initially, 2:1 ratio of $FeCl_3.6H_2O$ (0.002 mol) to $FeCl_2.4H_2O$ dissolved in 5 ml of HCl pH = 3-4). To adjust the pH = 11 the ammonia solution (2 M) was added to iron salts solution drop wise while vigorous stirring and under argon atmosphere. The solutions were purged by nitrogen gas for 10 min. The black precipitates were appeared and the mixture were heated to 80 °C. Three milliliters of Oleic acid were added to mixture and a black waxy precipitate formed. The mixture was then placed on permanent magnet and the supernatant was removed. Separated black waxy precipitate was washed 5 times with ethanol and then dispersed in 50 ml of n-hexane.

Preparation of Water-based Double Layer Functionalized IONPs

For preparation of DL-IONPs, 0.5 g CTAB and 0.5 g SDS dissolved in 20 ml double- distilled water, separately. Oleic acid coated IONPs (OA-IONPs) divided into two equal parts. In the following, 25 ml of OA-IONPs and 20 ml of CTAB solution were mixed and stirred for 24 h at room temperature and under N_2 gas. Same procedures was done with SDS. Synthesized water-based double layer functionalized IONPs (DL-IONPs) were separated with centrifugation and washed with water. Finally the prepared double layer coated iron oxide nanoparticles were dispersed in 50 ml double distilled water for subsequent experiments.

Characterization

For characterization of the DL-IONPs structure, the X-ray diffractometer X-ray diffraction (XRD, Broker AXS D8 Advance with Cu Kα radiation) was used. The particle size,

size distribution and zeta-potential (surface charge) of the synthesized DL-IONPs were determined by zeta sizer nano ZS, Malvern Company. Fourier transform infrared (FTIR) spectrum was recorded on FTIR spectrometer Bruker Tensor 27 and magnetization measurements were obtained at room temperature using a vibrating sample magnetometer (Lake Shore 7400 Vibrating Sample Magnetometer

Gel Retardation Assay

To assess the DNA condensation capability of DL-IONPs materials, a gel retardation assay was conducted. 2 µg of plasmid DNA was added to an equal volume of DL-IONPs solutions of indicated concentrations to achieve varying N/P ratios. Empty DL-IONPs materials and naked plasmid were used as controls. The samples were incubated at room temperature for 30 min before loading in a 1.5% agarose gel electrophoresis. Samples were electrophoresed through an agarose gel at 75 V for 1.0 h and stained with ethidium bromide to visualize the plasmid DNA. Non-condensated plasmids DNA were moved equal to the standard plasmid DNA, while the condensated plasmid DNA remained at loading well.

Cytotoxicity Assay

HEK 293 cells were seeded in 96-well plates for 5×10^3 cell per well using high-glucose DMEM supplemented with 10% fetal bovine serum (FBS) (GIBCO®EU 10270), and incubated for 24 h at 37 °C in humidified incubator with 5% CO_2 atmosphere. Different concentration of DL-IONPs materials was added to the cells and left for 48 h without exchanging the media. Then, 10 µl of MTT (5 mg ml^{-1}) was added to each well and the cells were incubated at 37 ℃ for 4 h. The formazan product was dissolved in 100 µl dimethyl sulfoxide (DMSO). Color intensity was measured using a micro plate reader at test and reference wavelengths of 570 nm.

Transfection Assay

HEK 293 cells were cultured in high-glucose DMEM supplemented with 10% fetal bovine serum (FBS), 100 U/ml penicillin and 100 g ml^{-1} streptomycin in humidified atmosphere of 5% CO_2 and 37 °C. Cells were seeded in a 60mm dishes on the cover slip for transfection studies. *HEK* 293 cells were seeded in the density of 1×10^5 per each cover slip and in the time of transfection they were 70-80% confluent. The cells were washed with PBS and the medium of each dish was replaced with 3 ml of the fresh medium (without serum) two hours preceding transfection. In this case, 1/1 ratio of DL-IONPs to DNA plasmid (*plasmid* with *GFP* coding sequence) were added to investigate transfection efficiency. After 4 h the media completely removed and cells were washed with PBS and complete media supplemented with 10% FBS was added to the cells and incubated for 24 and 48 h in humidified atmosphere of 5% CO_2 and 37 °C. The amount of produced *GFP* was used as a marker for monitoring transfection efficiency in *HEK* 293 cells, because the assay of this protein reporter is rapid and sensitive. To analyze *GFP*, the transfected cells on coverslip in each dish were gently washed with PBS. Finally, cover slips were mounted with Glycergel®(Dako, Barcelona, Spain) and analyzed by Axioplan2fluorescence microscope (Zeiss).

RESULTS AND DISCUSSION

In this work, in order to prepare DL-IONPs, initially iron oxide nanoparticles (magnetite, Fe_3O_4) were synthesized with wet chemistry and co-precipitation method. The possible reaction for the formation of Fe_3O_4 MNPs as follows:

$$Fe^{3+} + 3OH^- \rightarrow Fe(OH)_3$$

$$Fe(OH)_3 \rightarrow FeOOH + H_2O$$

$$Fe^{2+} + 2OH^- \rightarrow Fe(OH)_2$$

$$2FeOOH + Fe(OH)_2 \rightarrow Fe_3O_4\downarrow + 2H_2O$$

The reaction is rapid, very high yielding, and magnetite particles are seen immediately after addition of the iron salts. It is necessary the throughout reaction mixture be free of oxygen, otherwise magnetite can be oxidized to γ-Fe_2O_3 in the reaction medium [26]. Stability of magnetic nanoparticles (MNPs), as a gene or drug delivery tool in biomedical applications is an important parameter. The MNPs due to the Van der Waals forces and dipolar interactions, tend to agglomerate and can be stabilized,

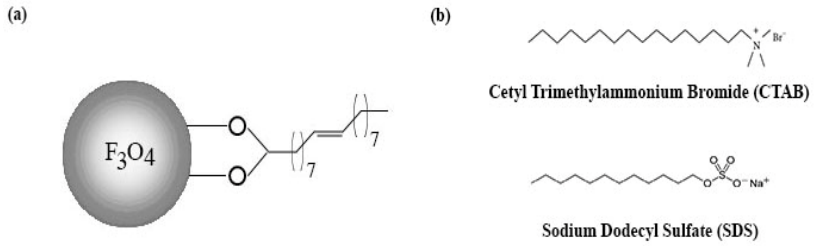

Fig. 1. (a) Super paramagnetic Iron Oxide Nanoparticles (SPIONPs) coated with oleic acid (b) structures of SDS and CTAB.

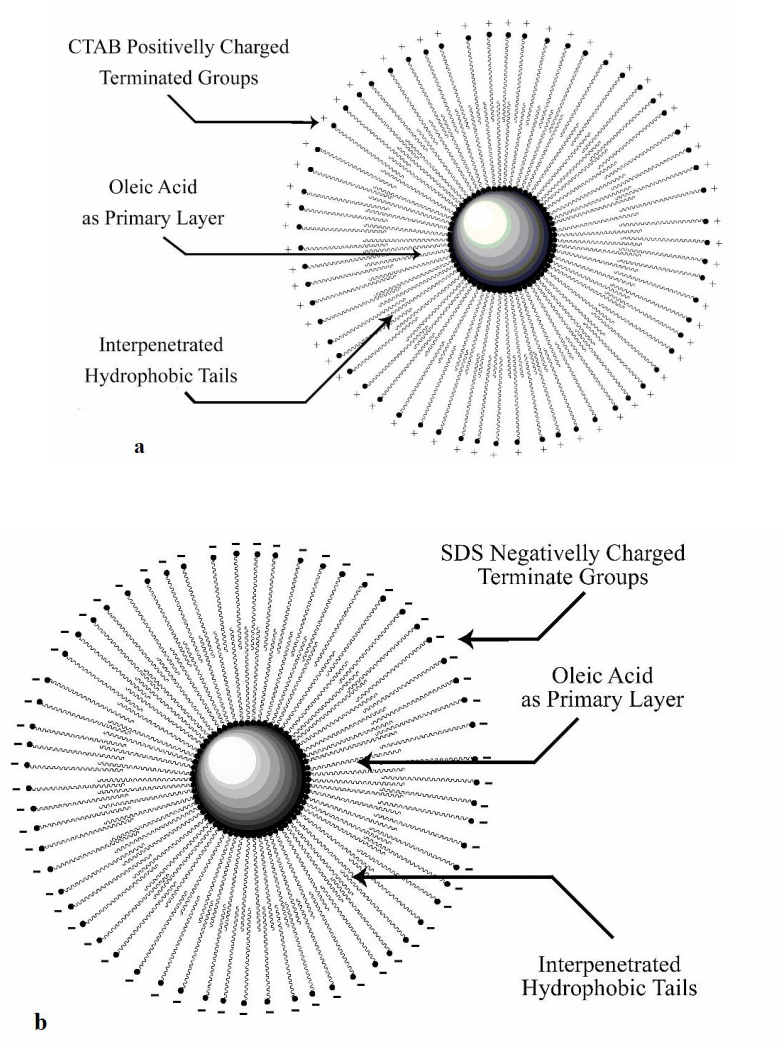

Fig. 2. Scheme of double layer coated magnetite nanoparticles with a) CTAB and Oleic Acid b) SDS and Oleic Acid.

through appropriate compounds. In the other hand, this coating can be used as a substrate for more functionalization and conjugation of biomolecules. Therefore, the addition of oleic acid (OA) to surface of IONPs both stabilizes and prepares an intermediating layer for subsequent functionalization. As shown in Fig. 1a, hydrophobic IONPs were formed *via* oleic acid coordination to Fe_3O_4 surface by the carboxylic acid group, so that the hydrophobic tail including hydrocarbon chain, remains free.

In the next step, with the aim of DL-IONPs preparation, a monolayer of surfactant was self-assembled around of the OA-IONPs whereas hydrophobic tails of SDS or CTAB interpenetrate in free tails of OA and consequently DL-IONPS are formed

Since in gene delivery and carrying negatively charged moieties, carriers with positive charge can carry more cargo than neutral or negatively charge ones. Using CTAB as the second layer, the terminate amine groups creates positive charge around the DL-IONPs. In this work, we were focused on DL-IONPs using CTAB and their ability to carrying and transfection of GFP-protein gene to HEK293 cells. Structures of SDS and CTAB are shown in Fig. 1b. Also, as shown in Fig. 2, in intermediate layer, which hydrophobic tails interpenetrates to each other, there is potential loading capacity for transporting hydrophobic drug.

Representative FT-IR spectra of naked Fe_3O_4 nanoparticles (a) and DL-IONPs coated by oleic acid and CTAB (b) are exhibited in Fig. 3. The absorption band at 3444 cm^{-1} is attributed to the stretching vibrations of O-H, which is assigned to surface OH groups of naked Fe_3O_4 NPs and is resulted from a reduced amount of water in the sample. The absorption band at 589 cm^{-1} in both the FTIR spectra (a) and (b) is relevant to the Fe-O bond and confirms the form of Fe_3O_4. By comparison Figs. 3a and b, we observed new adsorption bands at 1722 cm^{-1} corresponding to C=O group and 998 cm^{-1} representing stretching vibration of C=C bond of oleic acid. In addition, the absorption bands at 2863 and 2923 cm^{-1} are attributed to C-H stretching vibration of CTAB and oleic acid, and 1437 cm^{-1} is due to the scissoring vibration of methylene and the peck at 1380 cm^{-1} is attributed to C-N bond of CTAB [27]. Thus all peaks at FTIR spectra confirmed that the surface of Fe_3O_4 NPs was well modified by oleic acid and CTAB.

X-ray powder diffraction (XRD) analytical technique mainly was used to recognize the crystalline structure of the product. It was observed from the XRD pattern of synthesized nanoparticles was presented in Fig. 4, that the peaks at (220), (311), (400), (422), (511), (440) and (731) are relevant to the phase of Fe_3O_4 [28]. The XRD peak well matched with the characteristic peaks of inverse cubic spinel structure (JCPDS card No. 88-0315) [29]. The average crystallite size of magnetite nano-crystals (D), is determined from the Debye- Scherer equation [30], $D = K\lambda / (\beta \cos\theta)$, where K is a constant (K = 0.9 for Cu-Ka), λ is wavelength (0.15405 nm for Cu-Ka), β is the peak width of half-maximum and θ is the diffraction angle. Thus the crystallite size of modified Fe_3O_4 NPs obtained from this formula was about 15.4 nm.

Average size of DL-IONPs was measured and the corresponding size distribution was presented in Fig. 5. The average size and surface charge of these DL-IONPs were obtained 31.6 nm and 17.5 mV, respectively. With the intention study their magnetic behavior, vibrating sample magnetometry (VSM) were performed for magnetization measurement. Vibrating sample magnetometry as-prepared iron oxide nanoparticles exhibited a high saturation magnetization value of 80 emu g^{-1} (Fig. 6). Accordingly that observed in Fig. 6, the magnetization curve measured for magnetite nanoparticles at room temperature exhibited superparamagnetic behavior because of was not observed hysteresis, coercivity and remanence [31]. The higher magnetic saturation of DL-IONP builds it candidate for magnetic hyperthermia and biomedical application.

Investigation of DNA Binding Capability by Agarose Gel Retardation Assay

Gel retardation assay was performed to show the mobility of the plasmid and ability of DL-IONPs to loading of them. The gel retardation assay result has been shown in Fig. 7. DL-IONPs in three dilutions, concentrated (Fig. 7b), 10 times diluted with deionized water (Fig. 7c) and 100 times diluted with deionized water (Fig. 7d), which dissolved in HEPES buffer pH 7.4 was mixed with the plasmids. DL-IONPs and naked plasmid also were used as controls, Figs. 7f and 7a, respectively. As indicated in Fig. 7, DL-IONPs have the ability for loading the negatively

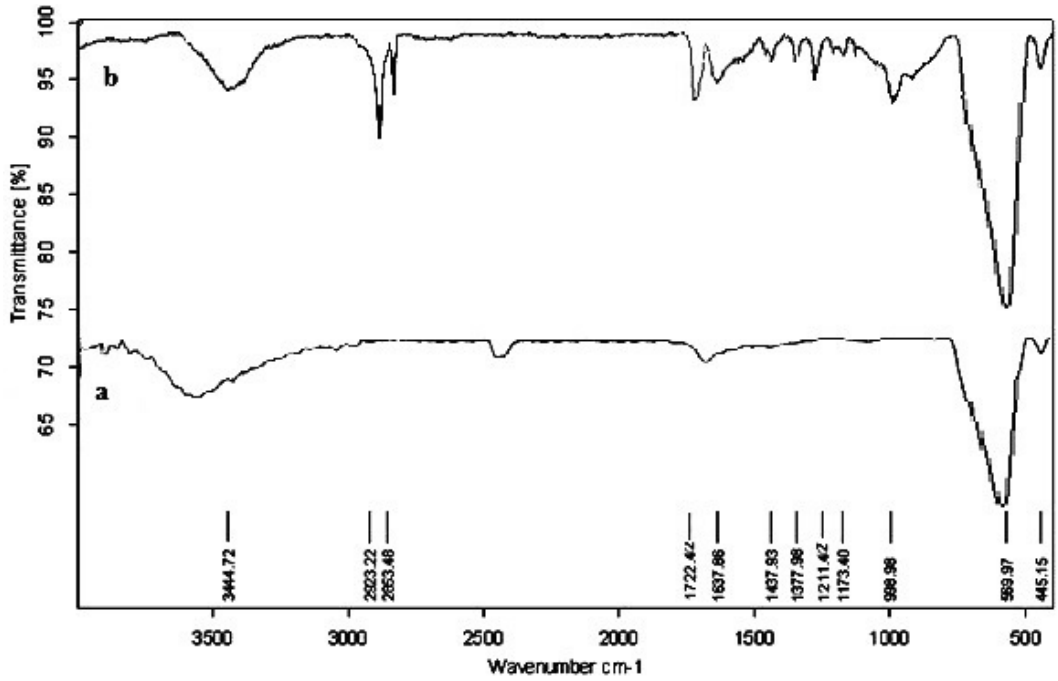

Fig. 3. FTIR spectra of (a) naked Fe_3O_4 nanoparticles (b) Fe_3O_4 nanoparticles treated by oleic acid and CTAB (DL-IONPs).

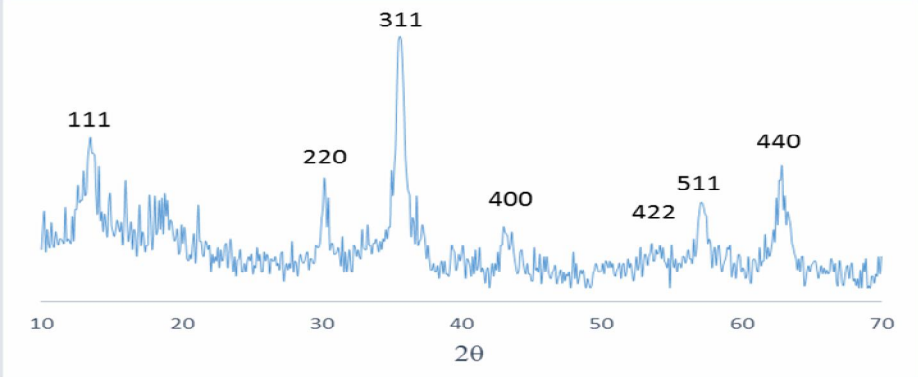

Fig. 4. XRD pattern of synthesized Magnetite Fe_3O_4 nanoparticles.

charged plasmids and with reducing the N/P ratio, the capability of plasmid loading remarkably reduce.

Evaluation of DL-IONPs Toxicity

In the mitochondria of living cells, the yellow tetrazolium MTT (3-(4,5-dimethylthiazolyl-2)-2,5-diphenyl-tetrazolium bromide) is reduced to purple formazan, by the action of dehydrogenase enzymes, to generate reducing equivalents such as NADH and NADPH. Toxicity is one of the most challenging areas in designing of a DL-IONPs. MTT assay was used to investigate the toxicity of DL-IONPs against HEK 293 cells at different concentrations of the DL-IONPs. HEK 293 cells were incubated with various amount of DL-IONPs for 24 h to examine the toxicity of the

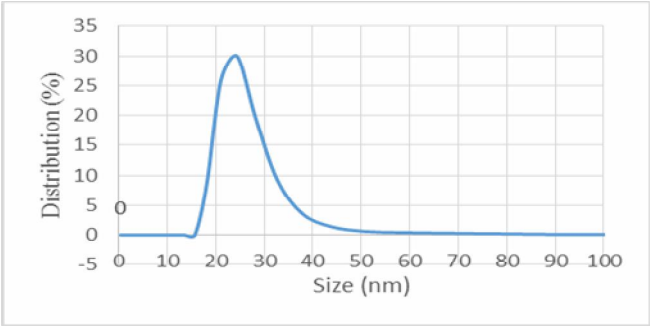

Fig. 5. Size distribution of DL-IONPs.

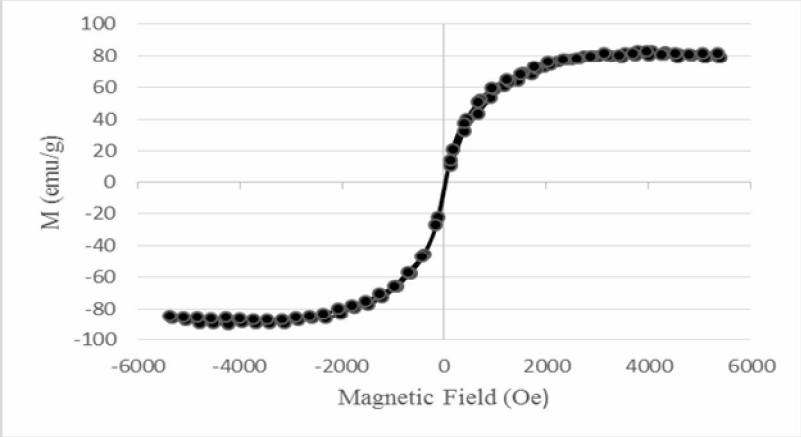

Fig. 6. Magnetization curve of DL-IONPs at room temperature.

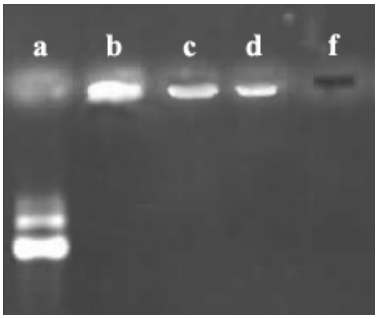

Fig. 7. 1.5% agarose gel electrophoresis retardation assay of DL-IONPs- plasmid complexes.

DL-IONPs during the exposure to the cells. As indicated in Fig. 8. The results, expressed as percentage of cytotoxicity *vs*. concentration of the DL-IONPs, indicate that DL-IONPs suspension with 0.001 percent concentration can be used as a suitable gene carrier.

Cell Transfection

According to the gel retardation assay results, the best

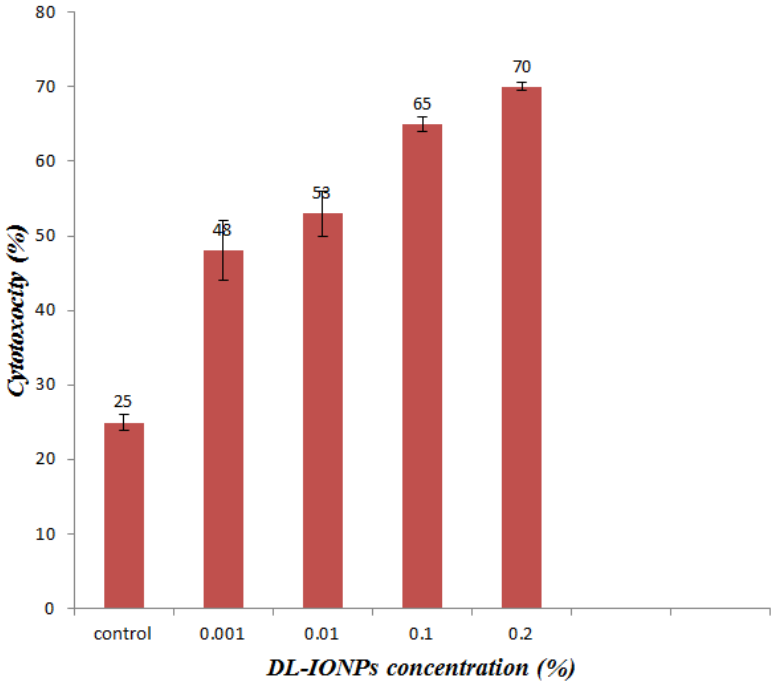

Fig. 8. Plot of percentage of cytotoxicity *vs*. concentration of the DL-IONPs against of the EK293 cell lines.

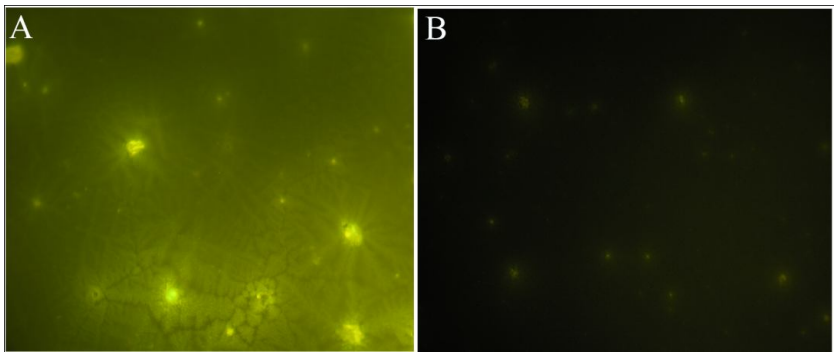

Fig. 9. GFP activity was measured 24 (A) and 48 (B) hours post-transfection.

DL-IONPs ratio for transfection was selected as N/P ratio = 1 and the efficacy of carrier for gene transferring was measured 24 and 48-hour post-transfection. Fluorescent images were acquired with an Axioplan2 fluorescence microscope (Ziess) using a filter with excitation at 490 nm and emission at 520 nm. As indicated in the Fig. 8, there was a significant difference between 24 h and 48 h post of incubation. This result probably related to protein degradation at longer incubation time.

CONCLUSIONS

The main aim of this study was to find an efficient and biocompatible carrier for delivering the genes into eukaryotic cells. For designing this carrier, the main challenge is related to the cell membrane and overcoming this barrier which can improve transfection efficiency. Results from gel retardation assay demonstrated that the DNA can efficiently attach to DL-IONPs particles, and

protect plasmid DNA from nucleases attack and degradation. Totally, it can be suggested that the current DL-IONPs may be a suitable carrier for gene delivery.

ACKNOWLEDGEMENTS

The authors gratefully acknowledge the funding support by Graduate University of Advanced Technology and Institute of Science, High Technology and Environmental Sciences (Project No. 7.2857).

REFERENCES

[1] a) G. Lin, H. Zhang, L. Huang, Mol. Pharmaceutics 12 (2015) 314; b) P.P. Kundu, V. Sharma, Curr. Opin. Solid State Mater. Sci. 12 (2008) 89; c) J.S. Choi, K. Nam, J. Park, J.B. Kim, J.K. Lee, J. Park, J. Controlled Release. 99 (2004) 445; d) Y. Wang, L. Zhang, S. Guo, A. Hatefi, L. Huang, J. Control. Release 172 (2013) 179.

[2] C. Mah, I. Zolotukhin, T.J. Fraites, J. Dobson, C. Batich, B.J. Byrne, Molecular Therapy 1 (2000) S239; b) C. Mah, T.J. Fraites, I. Zolotukhin, S. Song, T.R. Flotte, J. Dobson, C. Batich, B. J. Byrne, Molecular Therapy 6 (2002) 106; c) J. Dobson, Gene Therapy 13 (2006) 283; d) S.C. McBain, H. Yiu, J. Dobson, Int. J. Nanomedicine 3 (2008) 169.

[3] N.V. Jadhav, A.I. Prasad, A. Kumar, R. Mishra, S. Dhara, K. Babu, K.R. Babu, C.L. Prajapat, N.L. Misra, R.S. Ningthoujam, B.N. Pandey, R.K. Vatsa, Colloid Surface B: Biointerfaces 108 (2013) 158.

[4] C. Sun, J.S. Lee, M. Zhang, Adv. Drug Deliv. Rev. 60 (2008) 1252.

[5] S. Laurent, S. Dutz, U.O. Häfeli, M. Mahmoudi, Adv. Colloid Inter. Sci. 166 (2011) 8.

[6] C.S. Kumar, F. Mohammad, Adv. Drug Deliv. Rev. 63 (2011) 789.

[7] T.K. Jain, J. Richey, M. Strand, D.L. Leslie-Pelecky, C.A. Flask, V. Labhasetwar, Biomaterials 29 (2008) 4012.

[8] W. Wu, Q. He, C. Jiang, Nanoscale Res. Lett. 3(11) (2008) 397.

[9] K.E. Sapsford, W.R. Algar, L. Berti, K.B. Gemmill, B.J. Casey, E. Oh, M.H. Stewart, I.L. Medintz, Chem. Rev. 113 (2013) 1904.

[10] L.H. Reddy, J.L. Arias, J. Nicolas, P. Couvreur, Chem. Rev. 112 (2012) 5818.

[11] R. Massart, IEEE Transactions on Magnetics 17 (1981) 1247.

[12] Y. Han, D. Radziuk, D. Shchukin, H. Moehwald, Macromol. Rapid Commun. 29 (2008)1203.

[13] E. Hee Kim, H. Sook Lee, B. Kook Kwak, B.K. Kim, J. Magnetism and Magnetic Mater. 289 (2005) 328.

[14] K.V. Shafi, A. Ulman, A. Dyal, X. Yan, N.L. Yang, C. Estournes, L. Fournès, A. Wattiaux, H. White, M. Rafailovich, Chem. Mater. 14 (2002) 1778.

[15] A.B. Chin, I.I. Yaacob, J. Mater. Processing Technol. 191 (2007) 235.

[16] D.L. Thorek, A.K. Chen, J. Czupryna, A. Tsourkas, Annals of Biomed. Engin. 34 (2006) 23.

[17] J.L. Viota, F.J. Arroyo, A.V. Delgado, J. Horno, J. Colloid Inter. Sci. 344 (2010) 144.

[18] S. Ge, X. Shi, K. Sun, C. Li, C. Uher, J.R. Baker, B. Holl, J. Phys. Chem. C 113 (2009) 13593.

[19] S. Takami, T. Sato, T. Mousavand, S. Ohara, M. Umetsu, T. Adschiri, Mater. Lett. 61 (2007) 4769.

[20] V. Sreeja, P. Joy, Mater. Res. Bull. 42 (2007) 1570.

[21] J. Park, E. Lee, N.M. Hwang, M. Kang, S.C. Kim, Y. Hwang, J.G. Park, H.J. Noh, J.Y. Kim, J.H. Park , T. Hyeon, Angewandte Chemie 117 (2005) 2932.

[22] Y. Lu, Y. Yin, B.T. Mayers, Y. Xia, Nano Lett. 2 (2002) 183.

[23] F. Herranz, M. Morales, A.G. Roca, R. Vilar, J. Ruiz–Cabello, Contrast Media & Molecular Imaging 3 (2008) 215.

[24] C. Fu, N.M. Ravindra, Bioinspired, Biomimetic and Nanobiomaterials 1 (2012) 229.

[25] S. Laurent, D. Forge, M. Port, A. Roch, C. Robic, L. Vander Elst, R.N. Muller, Chem. Rev. 108 (2008) 2064.

[26] M. Mahdavi, M. Bin Ahmad, M.J. Haron, F. Namvar, B. Nadi, M. Zaki Ab Rahman, J. Amin, Molecules 18 (2013) 7533.

[27] a) M. Faraji, Y. Yamini, E. Tahmasebi, A. Saleh, F. Nourmohammadian, J. Iran. Chem. Soc. 7 (2010) S130; b) K. Khoshnevisan, M. Barkhi, Davood Zare, D. Davoodi, M. Tabatabaei, Metal-Org., Nano-Metal Chem. 42 (2012) 644.

[28] S. Sheng-Nan, W. Chao, Z. Zan-Zan, H. Yang-Long, S. S. Venkatraman, X. Zhi-Chuan, Chin. Phys. B 23 (2014) 037503.
[29] K. Sun, C. Sun, S. Tang, Cryst. Eng. Comm. 18 (2016) 714.
[30] Z. Li, H. Chen, H.B. Bao, M.Y. Gao, Chem. Mater. 16 (2004) 1391.
[31] M. Yamaura, R.L. Camilo, L.C. Sampaio, M.A. Macedo, M. Nakamura, H.E. Toma, J. Magn. Magn. Mater. 279 (2004) 210.